Scientific Research Publishing

Open Journal of Composite Materials, 2017, 7, 146-165
http://www.scirp.org/journal/ojcm
ISSN Online: 2164-5655
ISSN Print: 2164-5612

Nylon/Porphyrin/Graphene Oxide Fiber Ternary Composite, Synthesis and Characterization

César García-Pérez[1], Carmina Menchaca-Campos[1], Miguel A. García-Sánchez[2], Elsa Pereyra-Laguna[1], Ociel Rodríguez-Pérez[1], Jorge Uruchurtu-Chavarín[1]

[1]Centro de Investigación en Ingeniería y Ciencias Aplicadas-IICBA, Universidad Autónoma del Estado de Morelos, Cuernavaca, México
[2]Departamento de Química, UAM Iztapalapa, Vicentina, México
Email: cesar.garcia@uaem.mx

How to cite this paper: García-Pérez1, C., Menchaca-Campos, C., García-Sánchez, M.A., Pereyra-Laguna, E., Rodríguez-Pérez, O. and Uruchurtu-Chavarín, J. (2017) Nylon/Porphyrin/Graphene Oxide Fiber Ternary Compo-site, Synthesis and Characterization. *Open Journal of Composite Materials*, **7**, 146-165.
https://doi.org/10.4236/ojcm.2017.73009

Received: February 10, 2017
Accepted: July 4, 2017
Published: July 7, 2017

Abstract

This research was based on the manufacture of new composite materials that offer technological possibilities in the development of new devices with greater efficiency. Electrospinning was used to form nylon 66/-tetra-(para-aminophenyl) porphyrin ($H_2T(p\text{-}NH_2)PP$)/graphene oxide (GO) composite film. Graphene oxide coatings were obtained from graphite, through mechanical exfoliation followed by calcination and ultrasonic agitation in an oxidant solution. These samples were characterized under SEM, FTIR, Raman spectroscopy, UV-vis and R-X techniques. On the other hand, $H_2T(p\text{-}NH_2)PP$ was synthesized in two steps process by the Rothemun reaction and the Adler Method and it was integrated within nylon polyamide fibers by direct addition of a hexamethylenediamine/adipoyl chloride reactant mixture. The polymerization of the nylon/$H_2T(p\text{-}NH_2)PP$ species occurs in such a way that it starts or ends on the four peripherals-NH_2 groups, connected and located in the same molecular plane of $H_2T(p\text{-}NH_2)PP$, forming nylon chains at the periphery of the macrocycle. The association of GO with nylon/$H_2T(p\text{-}NH_2)PP$ fibers is performed by dipole-dipole interaction and hydrogen bonding. To take advantage of the properties of these materials, they were combined as a ternary composite.

Keywords

Electrospinning, Composite, Nylon, Porphyrin, Graphene Oxide

1. Introduction

The new developments in materials chemistry are applied to energy research and

nanoscience. The functional materials; composite and hybrid metal-organic porous structures developments are available for diverse applications, such as: hydrogen storage, carbon dioxide capture, the separation of fuel and toxic gases, and separation of hydrocarbon molecules.

Fibers have interesting properties such as high length to diameter ratio and hence find a lot of applications in various industries. The incorporation of fillers and nanofillers into electrospun fibers enhances its properties relevant to a number of applications, particularly mechanically reinforced composites [1]. The important properties of the fibers, which make them commercially important, are their small diameter, large surface area and small pore size, which are the ideal requirements for filtration, catalysis, and adsorption.

Graphene, a two dimensional allotrope of carbon separated from graphite in 2004 [2] [3] has attracted a lot of research interests due to its unique electronic structure and fascinating optical, thermal and chemical stability and mechanical properties [4] [5] [6]. Due to its excellent mechanical properties, graphene can be used in the formation of composite materials and reinforcement of fiber properties for improved performance; one of such properties is the thermal conductivity.

Among all possible aromatic molecules, synthetic tetrapyrrole macrocycles, such as porphyrins (H_2P) exhibit a wide range of interesting physico-chemical properties suitable to be used in high technology devices. Porphyrins are of primary interest in molecular electronics due to their rich electronic/photonic properties (including charge transport, energy transfer, light absorption or emission) [7]. The relatively easy synthesis and purification of substituted tetraphenyl porphyrins ($H_2T(S)PP$) make them very attractive for synthesize and preparation of systems applicable in diverse technological areas.

Most of polymeric materials are limited in their technological applications for their low conductivity and thermal stability, high electrical resistivity and plastic deformation. However, porphyrins and graphene oxide exhibits excellent properties which are seen to leverage incorporating them into polymeric matrixes to form a composite or hybrid material.

On the other hand, the properties that can be exploited from nylon are its high mechanical strength, stiffness, hardness and toughness. Combined with this polymer, the GO seeks to reduce the ionic and electrical resistance of the base material and improve its mechanical properties. In the same way porphyrin provides its coordination capacity, charge transport, energy transfer and light absorption or emission properties. These set of properties could be combined in hybrid materials and composites feasible to be used in innovative technological applications such as super-capacitors, organic solar cells, development of highly selective chemical sensors [8] [9], biological application as artificial muscles [10] [11] [12], proton exchange membrane, coating bipolar plates fuel cell, etc.

Electrospinning is one of the techniques for production of continuous fibers from micro to nanometer range by the application of electrostatic forces to a jetting polymer solution. The basic idea behind this technology dates back to the

early 1950's [13] [14] [15] [16]. Electrospinning is a very attractive technique for production of polymer fibers because of its simplicity, low cost, high productivity, reproducibility and its potential to be scaled up to industrial level [17]. The combination of graphene with the polymer, can improve the mechanical, electrical and thermal stability of the polymeric fibers [18] [19] [20].

2. Experimental

2.1. Graphene Oxide (GO)

The GO was obtained by the mechanical exfoliation of graphite (MEG). Subsequently, a series of treatments were performed to obtain the best GO conditions. Within these treatments there was a calcination in a muffle with an oxygen flow at a temperature of 700˚C for two hours to remove impurities (such as crystalline silica and silicates) and to obtain a greater separation of the sheets through its functionalization: a product of the graphite oxidation in the presence of oxygen, fixing it in the borders of the graphite sheets, achieving their separation. After that, ultrasonic agitation in peroxide solution was performed for six hours. Afterwards, the material were filtered, washed, and dried to obtain the GO.

2.2. Tetrakis-(Para-Aminophenyl) Porphyrin ($H_2T(p\text{-}NH_2)PP$

The free base of tetra-(para-aminophenyl) porphyrin, $H_2T(p\text{-}S)PP$, was synthesized in two step process by the Rothemun reaction and the Adler Method [21] from para-nitro benzaldehyde, pyrrole, and $Zn(Ac)_3$, under reflux in propionic acid (Figure 1). Once the reaction mixture was cooled, an equivalent volume of chloroform was added to the mixture, which was kept with ultrasonic agitation

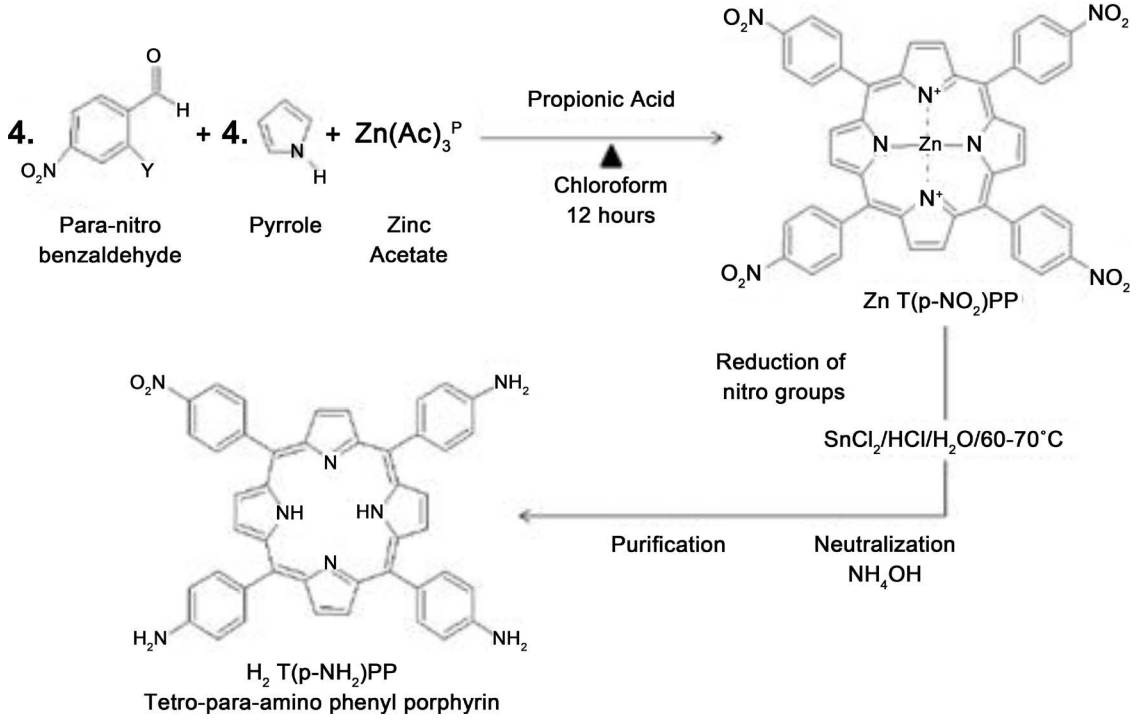

Figure 1. Synthesis route of $H_2T(p\text{-}NH_2)PP$ species.

for ten hours. The resultant dark purple solid was filtered and washed with methanol and chloroform. In a second step, the nitro groups (-NO_2) were reduced with $SnCl_2 \cdot 2H_2O$ to a temperature of 70˚C for 30 minutes. After, the mixture was neutralized with NH_4OH. A reddish precipitate of impure porphyrin was extracted from that solution with chloroform. Purified $H_2T(p\text{-}NH_2)PP$ solid was obtained through a chromatographic silica gel column.

2.3. Nylon/$H_2T(p\text{-}NH_2)PP$ Compound

To form the composite nylon/porphyrin it was required to prepare the next two solutions.

Solution A: Composed of a mixture of hexamethylene-diamine and sodium hydroxide in distilled water at 6.1% and 2.3%, respectively.

Solution B: Prepared with 2 ml of adipoyl chloride dissolved in 22 ml of chloroform, and the quantity desired of reacting porphyrin, which were 5 and 100 mg of $H_2T(p\text{-}NH_2)PP$ in the present work.

Once solutions were prepared, carefully hexamethylenediamine solution "A" was poured into adipoyl chloride and porphyrin solution "B". Immediately was observed the separation of solutions and the formation of nylon/$H_2T(p\text{-}NH_2)PP$ compound just at the interface of the two liquid volumes. The polymer formed at the interface is removed very slowly using tweezers, allowing contact and reaction of the two solutions to facilitate compound formation nylon/$H_2T(p\text{-}NH_2)PP$. Finally, the compound is washed with distilled water to remove traces of reagents and allowed to dry in an oven at 80˚C for 12 hours.

2.4. Nylon/H2T(p-NH2)PP/GO Compound

To form composite the nylon/$H_2T(p\text{-}NH_2)PP$ was dissolved in formic acid, and graphene oxide was added and the mixture was ultrasonicated at a temperature of 60˚C - 65˚C for 12 hours.

2.5. Electrospinning

The experimental setup system consists of three main parts: a controlled power source (Glassman High Voltage power source) providing a high voltage to create a high electrostatic field, an injector or perfusion pump (Srynge Pump Model NE300, 11 VDC Volts/Hertz, 0.75 Amperes) which generate pressure to a connected syringe and expelling the fluid and a stainless steel plate collector, where the polymer fibers are deposited.

The process starts with the preparation of a polymer solution. In the case of the nylon/GO, the weight percent of GO were 25% or 50% and for the nylon/$H_2T(p\text{-}NH_2)PP$ ratio, the percent of $H_2T(p\text{-}NH_2)PP$ were 0.1% or 1%. Additionally, for the nylon/$H_2T(p\text{-}NH_2)PP$/GO systems the weight percent of GO was set at 25% and for $H_2T(p\text{-}NH_2)PP$ were 0.1% or 1%.

All compounds were dissolved in formic acid and left stirring for 12 hours. The syringe (3 ml) is prepared by cutting and grinded the bevel part of the needle, which is electrically charged when connected to the power source.

Table 1. Electro-spinning parameters.

Composite	Charge (kV)	Flow Rate	Viscosity (cp)	Tip-Collector (cm)
Nylon	12	0.2 ml/h	122.24	15
Nylon/GO	12	0.4 µl/min	102.16	12
Nylon/Porphyrin	12	0.4 µl/min	101.86	12
Nylon/Porphyrin/GO	13	0.2 µl/min	106.96	12

In reported experiments, electrical charge is usually between 1 and 30 kV; other aspects taken into account are the flow rate and the distance between the needle tip and the collector. Distances in the range of 5 to 30 cm were evaluated in order to allowing the solvent to evaporate and the polymer fibers deposited on the collector [22] [23]. The electro-spinning process occurs because the electric force applied to the polymer solution, manages to overcome the surface tension of this, generating an electrically charged beam, which is exposed to the collector. When the fibers are dried, they are electrically charged and directly accelerated by electric forces on the collector (stainless steel 316), where they are deposited.

The electric charge, tip-collector distance and flow rate are parameters that were established to form the different composites shown in Table 1.

2.6. Characterization

Functionalized GO samples and electrodes were characterized using SEM, FT-IR, Raman spectroscopy, UV-Vis, R-X techniques and TGA.

2.6.1. Scanning Electron Microscopy

These tests were performed on a LEO model operating at 15 kV, at 1, 5, 10 and 15 kX resolution to determine size, form and distribution of GO flakes. Energy dispersive X-Ray spectroscopy (EDX) was used to determine the elemental chemical analysis of GO and to corroborate the presence of oxygenated functional groups and their distribution.

2.6.2. Infrared Spectroscopy (FT-IR)

With this technique was determined the change in the structure of the different compounds formed nylon/$H_2T(p\text{-}NH_2)PP$, nylon/GO and nylon/$H_2T(p\text{-}NH_2)PP$/GO in the frequency range 500 - 4000 cm^{-1}, 4 cm^{-1} resolution, in a spectrophotometer Model Vector 22 Bruker, equipped with OPUS 5.5 software.

2.6.3. Raman Spectroscopy

The used equipment: WITec alpha 300 AR, laser source: 532 nm (green) power: 15.6 mW, optical objective: 100X integration time: 5 s, accumulations number 8. This technique was used for the characterization of GO.

2.6.4. X-Ray Diffraction (XRD)

Patterns were recorded on a Bruker D2 PHASER diffractometer (35 kV, 20 m A, Japan) With Cu Ka radiation (λ = 1.548 Å) at a scan rate 2˚/min, in the 2θ angle range 5˚ to 30˚.

2.6.5. UV-Visible

UV-visible absorption spectra were recorded on Genesys 10S UV-Vis spectrophotometer and mainly used for the characterization of the $H_2T(p\text{-}NH_2)PP$.

2.6.6. Thermogravimetric Analysis (TGA)

Equipment: STA i 1000 (Simultaneous Thermal Analyzer) Instrument Specialists. Approximately 5 mg of sample was heated at a rate of 20˚C/min, in Nitrogen (N_2) atmosphere.

3. Results and Discussion

3.1. Scanning Electron Microscopy (SEM)

3.1.1. Nylon/$H_2T(p\text{-}NH_2)PP$ Compound

Figure 2 presents the result of electrospun polymer solution (nylon/porphyrin). The obtained fibers fall in the range of 700 - 800 nanometers of width, the image shows fibers in the range of 60 micrometers, forming a highly crossed network on the base material (collector).

3.1.2. Graphene Oxide Characterization

Figure 3 presents the results of the SEM characterization of the different treatments performed to MEG. A porous material is observed as a result of the thermal treatment, due to the elimination of impurities and desorption of CO_2 during its treatment at 700˚C for two hours (Figure 3(a) and Figure 3(b)). After the thermal treatment, a chemical treatment in peroxide solution was performed (Figure 3(c) and Figure 3(d)). Ultrasonic vibrations were applied in this process

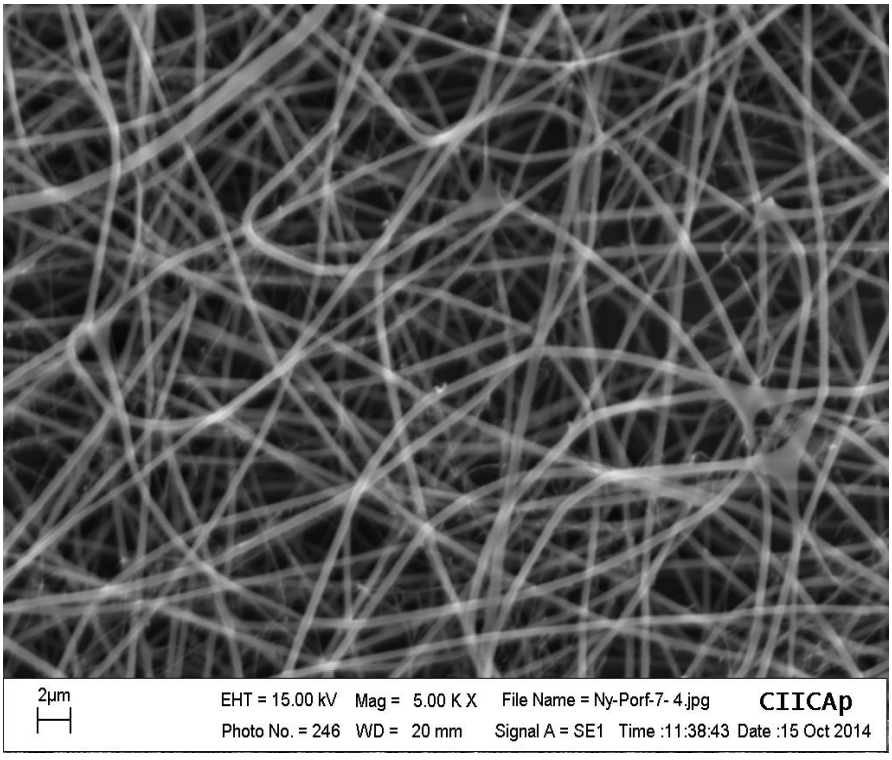

Figure 2. SEM micrograph of the nylon/$H_2T(p\text{-}NH_2)PP$ compound.

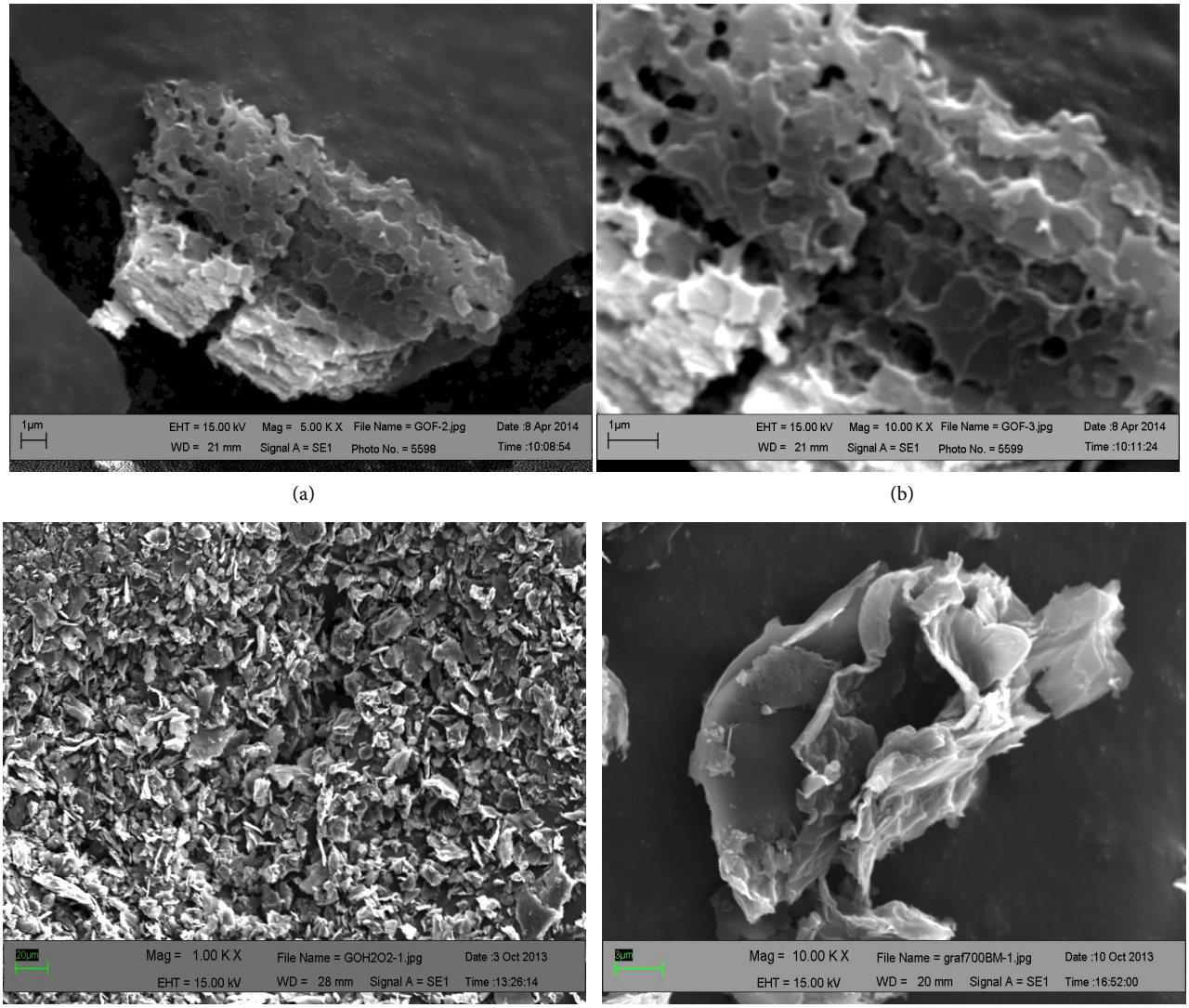

Figure 3. SEM images of MEG samples after different chemical or thermal treatment: (a) treated 700˚C to 5 kX; (b) treated 700˚C to 10 kX; (c) treated 700˚C and H_2O_2 to 1 kX and (d) treated 700˚C and H_2O_2 to 10 kX.

to facilitate the penetration of the oxidizing solution between the sheets and facilitate their separation. The combination of these processes results in a delaminated and low-dimensional material as seen in **Figure 3(c)**. These sheets are observed as slightly folded layers due to loss of planarity and as a result of their functionalization (**Figure 3(d)**).

3.1.3. SEM-EDX Graphene Oxide Characterization

A particle sample was characterized using SEM and EDX as can be seen in **Figure 4**. The chemical composition of a GO thin sheet (**Figure 4(a)**) was determined through energy dispersive X-rays (EDX), as seen in **Figure 4(b)**. Sheet characterization shows the presence of oxygen groups attached over a structure mainly constituted by carbon (**Figure 4(c)** and **Figure 4(d)**) respectively. The low oxygen percentage may be due to the weak peroxide oxidation process, compared to other chemical oxidation, such as the Hummer's process.

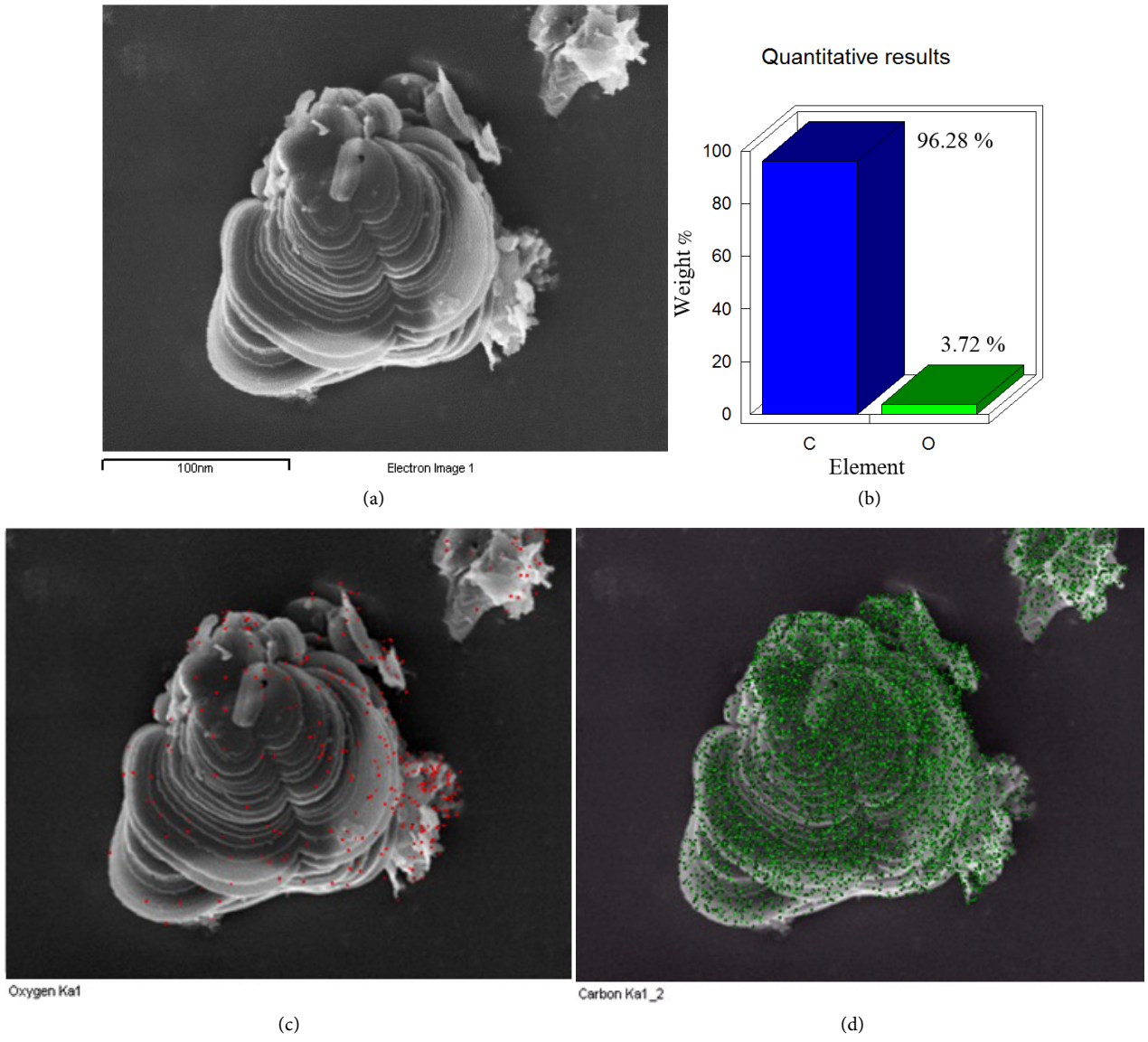

Figure 4. (a) SEM image of GO; (b) Characterized area through EDX and elemental mapping characterization shows the presence of: (c) oxygen groups (in red) and (d) carbon (in green) in the structure.

3.1.4. Nylon/$H_2T(p\text{-}NH_2)PP$/GO Compound

SEM micrographs show a general view and magnification of the coated system (**Figure 5**). In **Figure 5(a)** and **Figure 5(d)** it can be observed even distribution of GO sheets at a concentration of 25 and 50% on the polymer matrix nylon/$H_2T(p\text{-}NH_2)PP$, respectively. Moreover in **Figure 5(b)** and **Figure 5(e)** a complex network of nylon/$H_2T(p\text{-}NH_2)PP$/GO plates can be observed. In the micrograph of **Figure 5(c)** and **Figure 5(f)**, the presence of functionalized graphite oxide layers possibly bonded and surrounded by the nylon/$H_2T(p\text{-}NH_2)PP$ fibers is observed. This peculiar pathway suggests that the presence of hydrophilic groups in the surface, but preferably in the periphery of the GO layers, that makes possible its interaction with the amide groups (-CO-NH-) of the nylon/$H_2T(p\text{-}NH_2)PP$ fibers [24]. The nature of these species in the materials can be confirmed through the FT-IR spectroscopy.

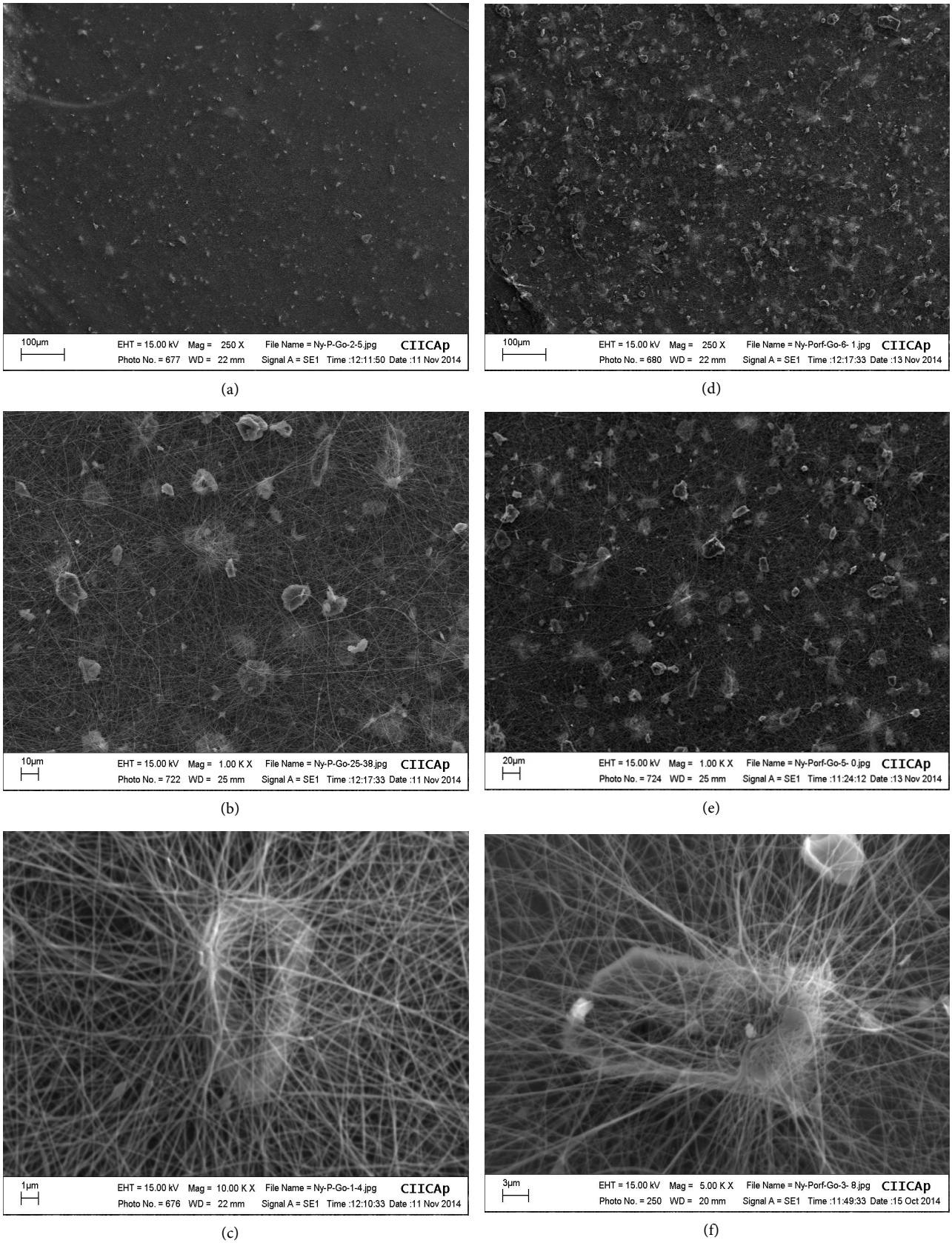

Figure 5. Nylon/$H_2T(p\text{-}NH_2)PP$/25% wt of GO compound: (a) 250 X; (b) 1 kX; (c) 10 kX and nylon/$H_2T(p\text{-}NH_2)PP$/50% wt of GO compound (d) 250 X; (e) 1 kX, (f) 5 kX.

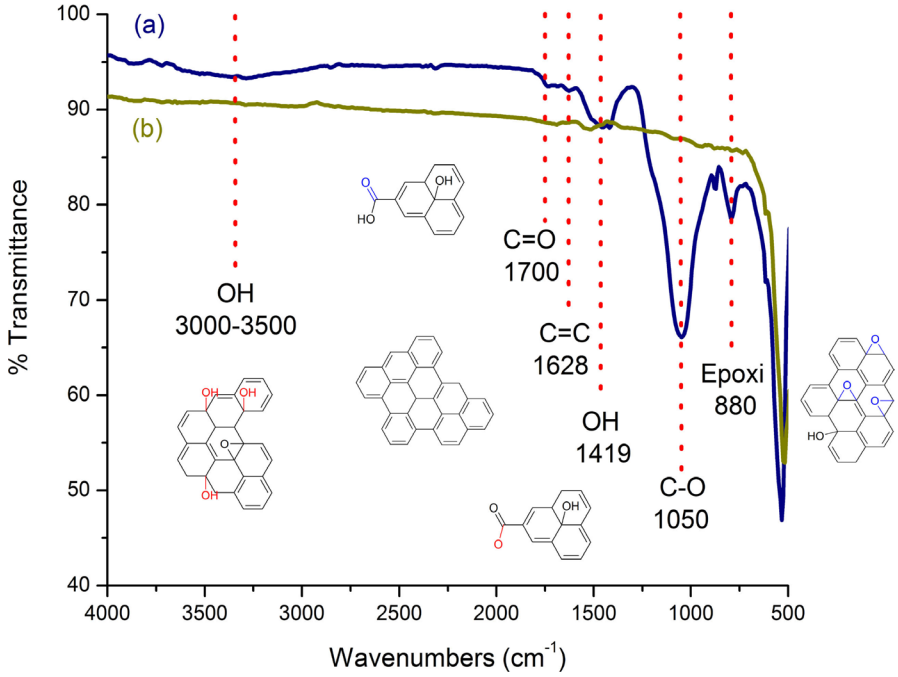

Figure 6. FT-IR spectra: (a) MEG after thermal and chemical treatment (GO) and (b) MEG blank.

3.2. Infrared Spectroscopy (FT-IR)

3.2.1. Graphene Oxide Characterization

The material structural changes was observed with this analysis and compared between the different compounds formed and MEG blank (**Figure 6**).

Figure 6 presents the spectrum obtained for the MEG after its thermal and chemical treatment in hydrogen peroxide showing bands that according to the literature [25] are characteristics of GO, as are the bands associated with stretching and flexion of the OH bond around 3000 - 3500 cm^{-1} and 1419 cm^{-1} respectively, the band near 1700 cm^{-1} is due to the presence of the C=O bond of the carbonyl group formed at the edges of the GO sheets, similarly, a band around 1628 cm^{-1} which corresponds to the stretching vibration of the C=C bond due to the presence of conjugated double bonds in the GO aromatic structure is also present, another band at 1050 cm^{-1} corresponding to the vibration of the C-O bond. Also a band that was observed at 880 cm^{-1} attributed to the C-O-C bond of the epoxy group. The functionalization and the change of hybridization of sp^2 to sp^3 of some of the oxidized carbons is a consequence of the loss of planarity, which induces the penetration of the oxidizing solution making possible the separation of some sheets.

3.2.2. FT-IR Composite Films Characterization

The FTIR spectrum of $H_2T(p\text{-}NH_2)PP$ free base species (**Figure 7**), presents one band that can be seen at around 3300 cm^{-1} and another one at 960 cm^{-1}; these signals can be ascribed to the NH bond stretching and bending frequencies of NH_2 substituents and of the central nitrogens of the macrocyclic porphyrin free bases. The bands located in the range from 2850 to 3150 cm^{-1}, are attributed to

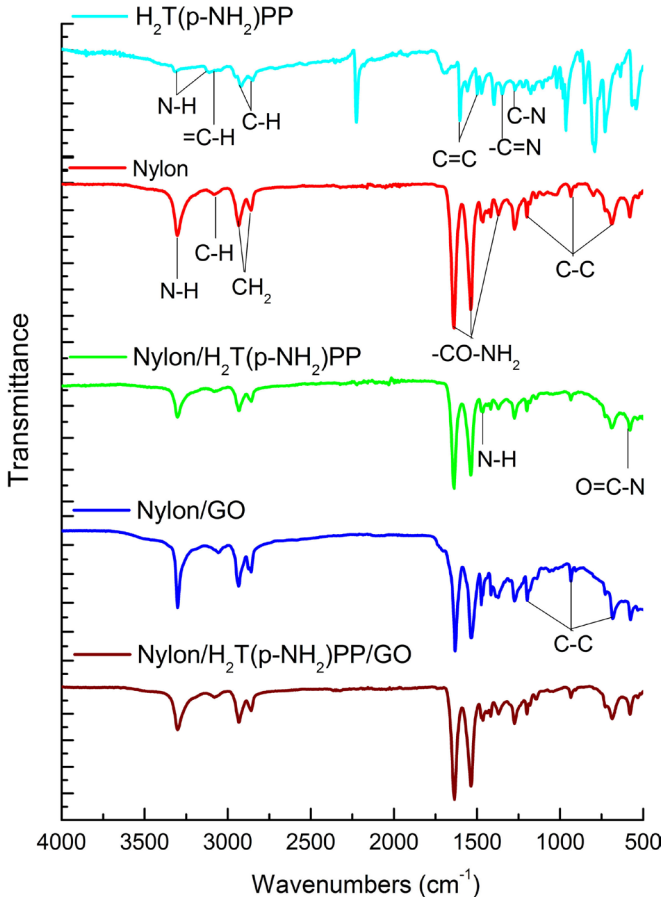

Figure 7. FTIR spectra of $H_2T(p\text{-}NH_2)PP$ free base, nylon 66 (blank), nylon/$H_2T(p\text{-}NH_2)PP$, nylon/GO and nylon/$H_2T(p\text{-}NH_2)PP$/GO composites.

C-H bond vibrations of the benzene and pyrrole rings.

The band located at around 1490 to 1650 cm^{-1} can be assigned to C=C vibrations and that located at around 1350 and 1272 cm^{-1} can be due to –C=N and C-N stretching vibrations. The signals at around 1800 to 1900 cm^{-1} as well as the bands at about 800 cm^{-1} and 750 cm^{-1} are attributed to C-H bond bending vibrations of para-substituted phenyls.

In the FTIR spectra of pure nylon 66 it can be observed that the bands at 3314 and 3221 cm^{-1}, and those arising at 1450 cm^{-1} and 750 cm^{-1} which can be assigned to the stretching, deformation, and wagging vibrations of N-H bonds. The bands at 2946 and 2867 cm^{-1} are associated to the CH_2 stretching vibrations. In turn, the C=O stretching vibrations can be observed at around 1717 cm^{-1}. The stretching, asymmetric deformation and wagging of NH amide groups are observed at 1654, 1547, and 1376 cm^{-1}, respectively. The bands located at around 1140 cm^{-1} can be attributed to CO-CH symmetric bending vibration combined with CH_2 twisting. The bands at 936, and 600 cm^{-1} are associated with the stretching and bending vibrations of C-C bonds, and the band at 583 cm^{-1} can be due to O=C-N bending. Additionally, the bands appearing at 936 and 1140 cm^{-1} are associated to the crystalline and amorphous structures of nylon 66, respectively [26].

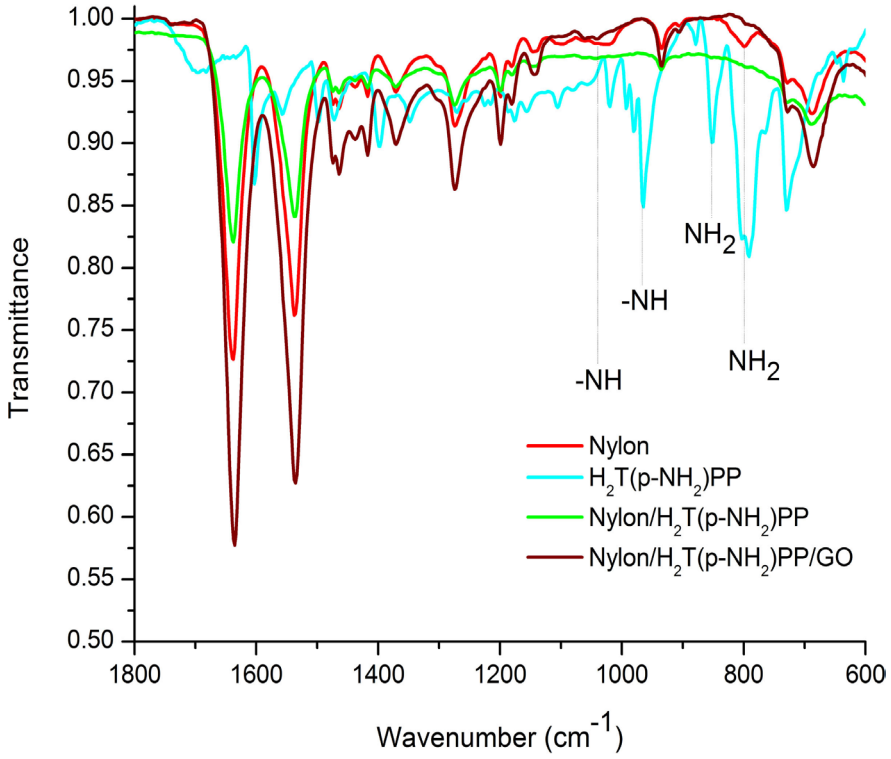

Figure 8. FTIR, spectra amplification of the different compounds at wavelengths of 1800 - 600 cm^{-1}.

In the spectra of nylon/H_2T(p-NH_2)PP and nylon/H_2T(p-NH_2)PP/GO composites of Figure 8, as well as the nylon/GO samples of the Figure 7 the characteristics bands of these materials can be observed. Comparison of the different compounds with the base material (nylon 66) allows seeing small bands that disappear at 1100, 1030 and 800 cm^{-1}, corresponding to primary (NH_2) and secondary (-NH-) amines; likewise, the disappearance of other bands in the spectra of the different compounds is observed. In the spectrum of the porphyrin the bands associated to the -NH group appears at wavelength of 966 cm^{-1} and those attributed to the stretching vibrations of the NH_2 substituents are located at around 850 and 793 cm^{-1}. The absence of the aforementioned bands could be caused by the interaction between the base material (nylon 66), porphyrin (H_2T(p-NH_2)PP), or inclusively by the reaction of periphery amine groups of these last species, and the functional groups present on the periphery of the GO sheets, mainly carboxyl (COOH) or carbonyl (C=O) groups.

3.3. Raman Spectroscopy

Figure 9 shows data obtained from Raman spectroscopy; where it can be seen that there is a significant difference between the vibrational bands G, D and 2D mainly, these results confirm the graphitic structure.

The G band makes reference to sp^2 hybridization, and as this is characteristic of the structure of graphene, it is well defined throughout the process as observed.

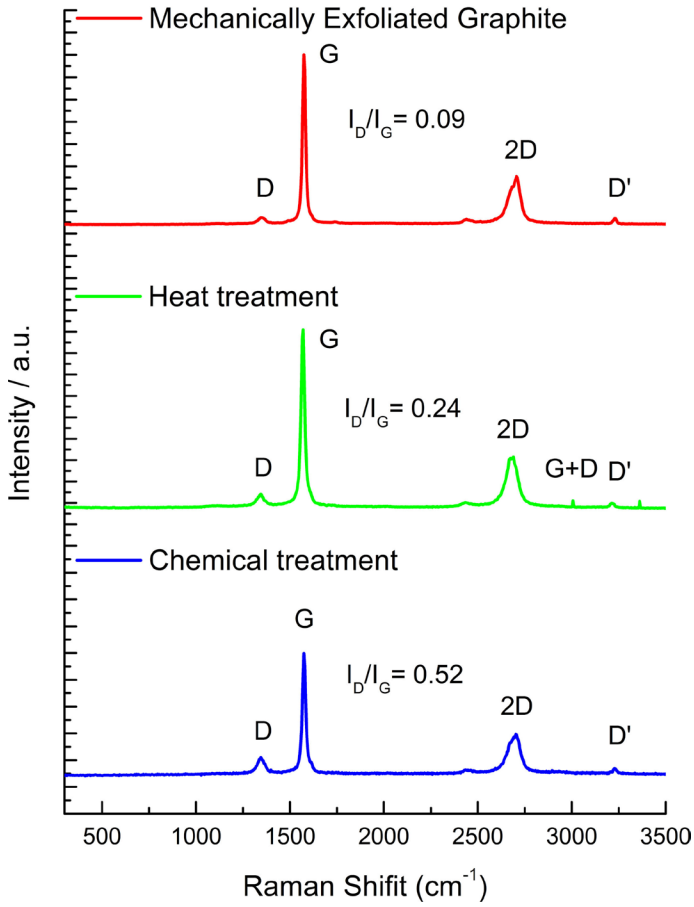

Figure 9. Raman spectra at 532 nm for different treatments in obtaining the GO.

Low D band intensities suggest that the graphene flakes contain few defects, predominantly located at the edges, compared with the basal plane of the flakes [27]. The intensity ratio of D to G (I_D/I_G) is different for each of the treatments performed to graphite, been 0.09 for graphite exfoliated mechanically, 0.24 for thermal treatment and 0.52 for the chemical treatment with hydrogen peroxide. These values are much lower than the GO obtained by other methods (1.2 - 1.5) further indicating high preservation graphene structure in the derivate GO samples [28] [29].

The 2D band is a frequency characteristic of the symmetry of graphene oxide, and denotes that as it is advanced in treating this, is becoming more defined but not completely enough. The shape of the 2D band is indicative of aggregation of thin layers in a so called multilayer (<5 layers).

3.4. X-Ray Characterization

The X-ray diffraction (DRX) was performed in the 2θ angle range between 5˚ to 30˚, due to the presence in that range of diffraction bands characteristic of the materials used in the synthesis of the composites.

3.4.1. GO X-Ray Diffraction

The X-ray diffraction (DRX) is a very useful tool to confirm the degree of

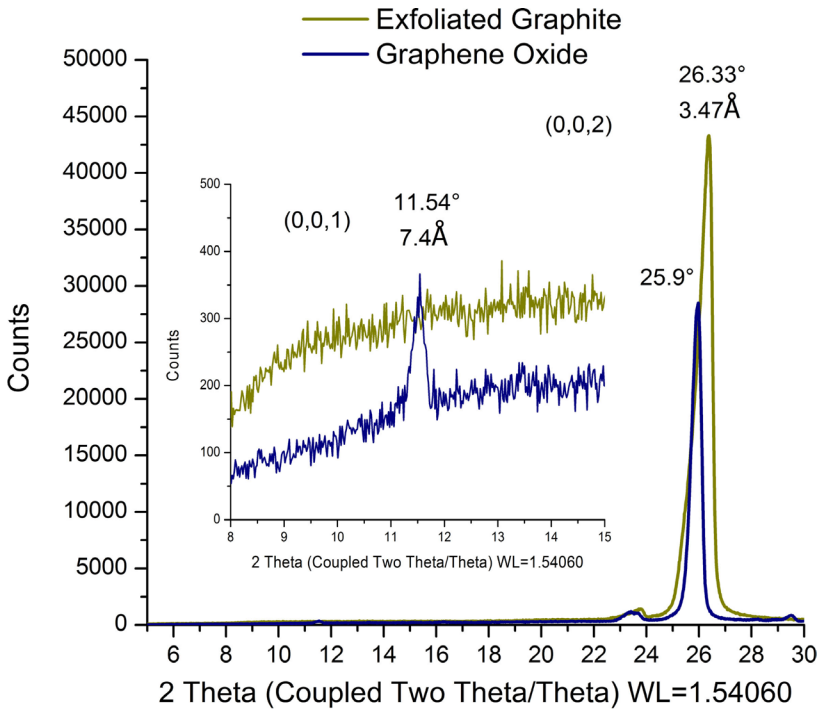

Figure 10. Ray-X diffraction spectra of graphene oxide and exfoliated graphite.

oxidation of graphite, since it involves the partial or complete separation of the signal (002) graphite in the diffractogram, and the appearance of a new (001) to $2\theta = 10^{\circ}$. Similarly it allows to follow the reduction of GO, since the signal (001) moves back, being closer to the starting graphite (26.5˚).

Once oxidized graphite, a material exhibiting functional groups containing oxygen is obtained, the functionalization of the material occurs mainly in the borders of the graphite, causing the distance between sheets to increase considerably. This phenomenon can be seen reflected in the diffractogram of graphene oxide **Figure 10**, by a slight displacement in the diffraction angle compared with the blank and a decrease in intensity signal, as well as the formation of a band to a diffraction angle 2θ of 11.54˚ corresponding to (001) plane. This indicates an increase in the separation of the layers of 7.4 Å, characteristic of GO determined from Bragg's law [30] [31].

3.4.2. Compounds X-Ray Diffraction

The X-ray diffraction patterns (**Figure 11**) of the nylon 66, nylon/H_2T(p-NH_2)PP, nylon/GO and nylon/H_2T(p-NH_2)PP/GO samples show the same diffraction pattern of a predominant amorphous material with some crystallinity. In this sense, the bands at around 20.47˚ and 23.56˚ correspond to the reflection of (100) and (010, 110) of the α phase of nylon 66 crystals oriented in a triclinic cell. The α^1 phase corresponds to the distance between adjacent chains of nylon 66, interacting through hydrogen bonding, while the α^2 phase is attributed to the distance between lamellae of polymer. The couple of bands attributed to the α phase were more intense for nylon/H_2T(p-NH_2)PP sample than for the pristine nylon 66. This difference in the nylon/H_2T(p-NH_2)PP sample could be

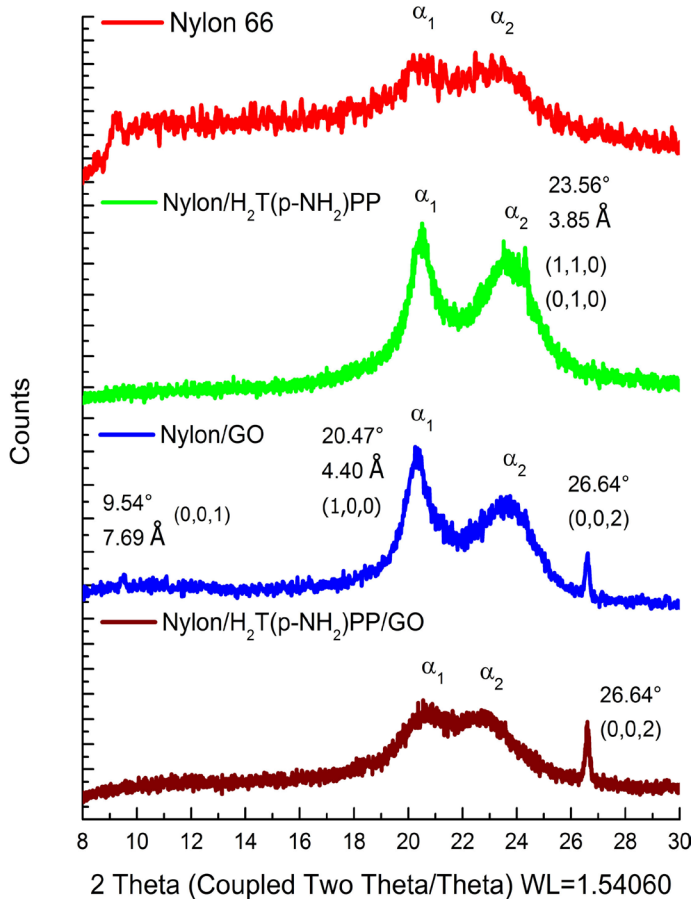

Figure 11. X-ray diffraction of the compounds: Nylon 66, nylon/$H_2T(p\text{-}NH_2)PP$, nylon/GO and nylon/$H_2T(p\text{-}NH_2)PP$/GO.

attributed to a slightly crystallinity increment induced by the incorporation of the porphyrin in the polyamide network [32].

The diffraction pattern of X-Ray of the compounds nylon/GO and nylon/$H_2T(p\text{-}NH_2)PP$/GO show bands at a diffraction 2θ angle of 26.64˚ and 9.54˚ in the case of composite nylon/GO, bands that are characteristic of graphene oxide, as can be seen in **Figure 10**.

3.5. UV-Vis Characterization

3.5.1. $H_2T(p\text{-}NH_2)PP$ Characterization

The UV-Visible spectra of porphyrins are characterized by an intense band at around 420 - 430 nm (Soret band) and four small Q bands in the range of 500 to 700 nm. These last signals are assigned to the $a_{2u} \rightarrow e_g$ and a_{1u}, $a_{2u} \rightarrow e_g$ electronic transitions, respectively [33]. In the case of the $H_2T(p\text{-}NH_2)PP$ specie, the Soret band is located at 427 nm, while four bands appearing at 522, 560, 590 and 654 nm (**Figure 12**), which is characteristic for the monomers of a porphyrin free bases. In acid solution, the purple-red solution of these compounds turns green as a consequence of the protonation of the central nitrogens of the porphyrin macrocycle that leads to the formation of the slightly nonplanar $H_4T(p\text{-}NH_2)PP^{2+}$ dicationic specie.

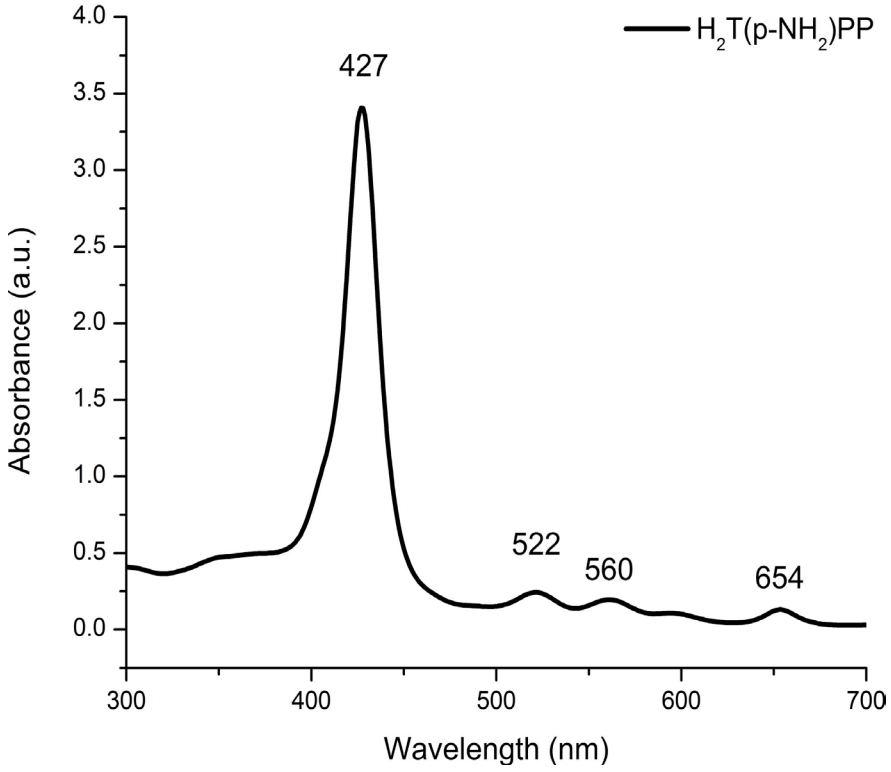

Figure 12. UV-Vis spectrum of the synthesized $H_2T(p\text{-}NH_2)PP$ free bases.

3.5.2. Nylon/$H_2T(p\text{-}NH_2)PP$/GO Characterization

In the visible UV absorption spectra of the nylon/$H_2T(p\text{-}NH_2)PP$/GO system an absorption peak at 280 nm assigned to the π-π* transition of the aromatic C=C bond is observed (**Figure 13**), present in the structure of GO as in that of the porphyrin. Also, an absorption peak at 427 nm representing Soret or B band, characteristic of porphyrins is observed overlapped to the spectrum of the GO.

3.6. TGA Characterization

Figure 14 shows the TGA results generated on nylon 66, $H_2T(p\text{-}NH_2)PP$, nylon/$H_2T(p\text{-}NH_2)PP$, nylon/GO and nylon/$H_2T(p\text{-}NH_2)PP$/GO.

The TGA results show that the nylon 66 polymer and $H_2T(p\text{-}NH_2)PP$ undergo thermal degradation beginning at 148˚C, on the other hand nylon/$H_2T(p\text{-}NH_2)PP$, nylon/GO and nylon/$H_2T(p\text{-}NH_2)PP$/GO compounds show an increase in temperature in the first thermal degradation at 305˚C, as consequence of the chemical interaction between nylon, $H_2T(p\text{-}NH_2)PP$ and GO, going from a linear nylon chain to a branched chain. Similarly a gradual thermal degradation is observed, starting when remains around 70% of total mass of the composites that included the GO, surely because the nylon and nylon/$H_2T(p\text{-}NH_2)PP$ fibers are interacting with the edges of GO sheets.

3.7. Structure

All the above mentioned tests suggest a chemical interaction between the different materials that make up the compound, in the case of the species ny-

lon/$H_2T(p\text{-}NH_2)PP$ the polymerization occurs in such a way that it starts or ends on the four peripherals -NH_2 groups, connected and located in the same molecular plane of $H_2T(p\text{-}NH_2)PP$, forming nylon chains at the periphery of the macrocycle [32]. In the presence of $H_2T(p\text{-}NH_2)PP$ the polyamide chain formation take place faster; this polymerization is favored due to the lower basicity

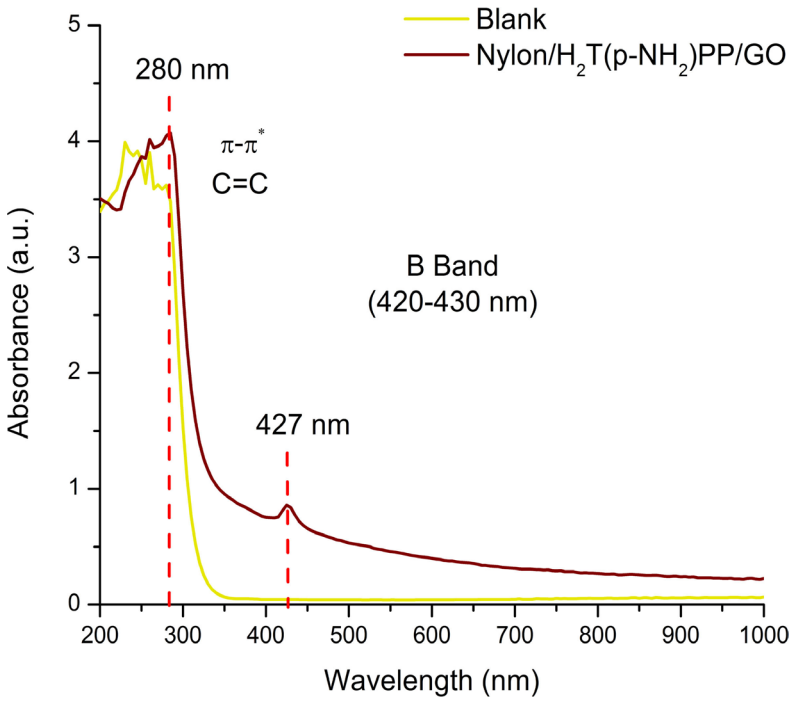

Figure 13. UV-Vis spectra of the system: Nylon/$H_2T(p\text{-}NH_2)PP$/GO.

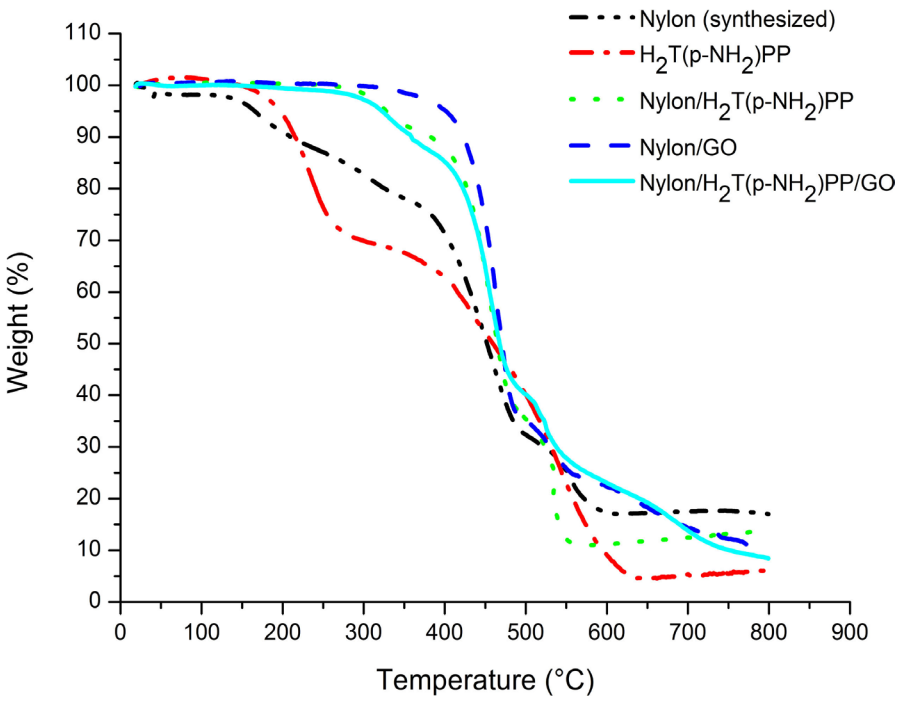

Figure 14. TGA results obtained for nylon 66, $H_2T(p\text{-}NH_2)PP$, nylon/$H_2T(p\text{-}NH_2)PP$, nylon/GO and nylon/$H_2T(p\text{-}NH_2)PP$/GO showing thermal degradation.

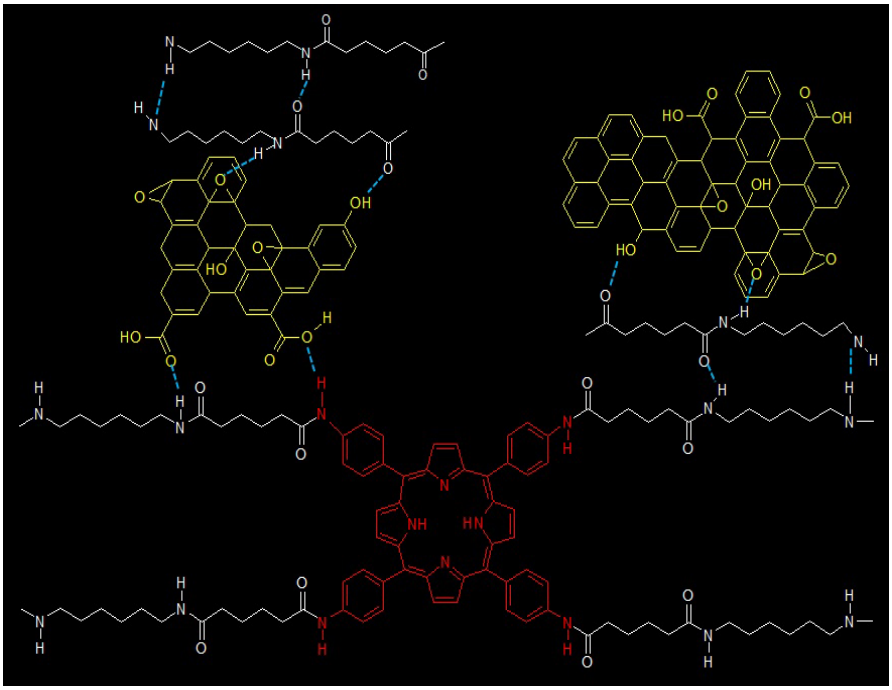

Figure 15. Chemical structure of the nylon/$H_2T(p\text{-}NH_2)PP$/GO compound, dipole-dipole interactions and hydrogen bonds between the different species.

of the -NH_2 groups present in the periphery of $H_2T(p\text{-}NH_2)PP$, compared with the basicity of these same groups in hexamethylenediamine. Dipole-dipole interactions and hydrogen bonds of nylon amide groups are mainly responsible for the structure of the polyamide network formed with the $H_2T(p\text{-}NH_2)PP$ species, in the same way, these interactions participate in the union of the compound nylon/$H_2T(p\text{-}NH_2)PP$ with GO sheets, mainly between the amide groups of the polyamide and carbonyl (C=O) or carboxyl (-COOH) groups, located in the periphery of the GO sheets (Figure 15).

4. Conclusions

Composites nylon/$H_2T(p\text{-}NH_2)PP$, nylon/GO and nylon/$H_2T(p\text{-}NH_2)PP$/GO were developed by electrospinning technique. Their characterization suggests high level of interaction and integration between the compounds of the composite, mainly between the compound nylon/$H_2T(p\text{-}NH_2)PP$ and the GO appearing preferentially in the periphery of the GO sheets, improving properties such as thermal degradation.

These interactions between the materials are intended to be used, for use in technological applications in the area of energy.

References

[1] Ramakrishna (2005) An Introduction to Electrospinning and Nanofibers. World Scientific Publishing, Sinapore City.

[2] Geim, A.K. and Novoselov, K.S. (2007) The Rise of Graphene Nat. *Mater*, **6**, 183-191.

[3] Novoselov, K.S., Geim, A.K., Morozov, S.V., Jiang, D., Katsnelson, M.I., Grigorieva, I.V., *et al.* (2005) Two-Dimensional Gas of Massless Dirac Fermions in Graphene. *Nature*, **438**, 197-200. https://doi.org/10.1038/nature04233

[4] Otsuki, J. (2010) STM Studies on Porphyrins. *Coordination Chemistry Reviews*, **254**, 2311-2341. https://doi.org/10.1016/j.ccr.2009.12.038

[5] Bobacka, J., Ivaska, A. and Lewenstam, A. (2003) Electranalysis. John Wiley & Sons, Hoboken, 366.

[6] Michalska, A., Nadrzycka, U. and Maksymiuk, K. (2001) Study of Polypyrrole Film as Redox Electrode. *Analytical Chemistry*, **371**, 35. https://doi.org/10.1007/s002160100926

[7] Holzhauser, P., Bouzek, K.J. (2006) Influence of Counter-Ions on the Permeability of Polypyrrole Films to Hydrogen. *Journal of Applied Electrochemistry*, **36**, 703. https://doi.org/10.1007/s10800-006-9132-0

[8] Weidlich, C., Mangold, K.M. and Juttner, K. (2001) Conducting Polymers as Ion-Exchangers for Water Purification. *Electrochimica Acta*, **47**, 741. https://doi.org/10.1016/S0013-4686(01)00754-X

[9] Wang, J. (2000) Analytical Electrochemistry. Wiley-VCH, New York. https://doi.org/10.1002/0471228230

[10] Hermann, A., Chaudhuri, T. and Spagnol, P. (2005) Bipolar Plates for PEM Fuel Cells: A Review. *International Journal of Hydrogen Energy*, **30**, 1297-1302. https://doi.org/10.1016/j.ijhydene.2005.04.016

[11] Davies, D.P., Adcock, P.L., Turpin, M. and Rowen, S.J. (2000) Bipolar Plate Materials for Solid Polymer Fuel Cells. *Journal of Applied Electrochemistry*, **30**, 101-105. https://doi.org/10.1023/A:1003831406406

[12] Wang, H., Sweikart, M.A. and Turner, J.A. (2003) Stainless Steel as Bipolar Plate Material for Polymer Electrolyte Membrane Fuel Cells. *Journal of Power Sources*, **115**, 243-251. https://doi.org/10.1016/S0378-7753(03)00023-5

[13] Formhals, A. (1934) Process and Apparatus for Preparing Artificial Threads. US Patent No. 1975504.

[14] Formhals, A. (1939) Method and Apparatus for Spinning. US Patent No. 2160962.

[15] Formhals, A. (1940) Artificial Thread and Method of Producing Same. US Patent No. 2187306.

[16] Formhals, A. (1943) Production of Artificial Fibers from Fiber Forming Liquids. US Patent No. 2323025.

[17] Novoselov, K.S., Geim, A.K., Morozov, S.V., Jiang, D., Zhang, Y., Dubonos, S.V., *et al.* (2004) Electric Field Effect in Atomically Thin Carbon Films. *Science*, **306**, 666-669. https://doi.org/10.1126/science.1102896

[18] Kim, H., Miura, Y. and Macosko, C.W. (2010) Graphene/Polyurethane Nanocomposites for Improved Gas Barrier and Electrical Conductivity. *Chemistry of Materials*, **22**, 3441-3450. https://doi.org/10.1021/cm100477v

[19] Senguptaa, R., Bhattacharyaa, M., Bandyopadhyayb, S. and Bhowmicka, A.K. (2011) A Review on the Mechanical and Electrical Properties of Graphite and Modified Graphite Reinforced Polymer Composites. *Progress in Polymer Science*, **36**, 638-670. https://doi.org/10.1016/j.progpolymsci.2010.11.003

[20] Du, J. and Cheng, H.-M. (2012) The Fabrication, Properties, and Uses of Graphene/Polymer Composites. *Macromolecular Chemistry and Physics*, **213**, 1060-1077. https://doi.org/10.1002/macp.201200029

[21] Adler, A.D., Longo, F.R., Finarelli, J.D., Goldmacher, J., Assour, J. and Korsakoff, L.

(1967) A Simplified Synthesis for Mesotetraphenyl-Porphyrin. *Journal of Organic Chemistry*, **3**, 476-476. https://doi.org/10.1021/jo01288a053

[22] Yarin, A.L., Koombhongse, S. and Reneker, D.H. (2001) Taylor Cone and Jetting from Liquid Droplets in Electrospinning of Nanofibers. *Journal of Applied Physics*, **90**, 4836-4846. https://doi.org/10.1063/1.1408260

[23] Shin, Y.M., Hohman, M.M, Brenner, M.P. and Rutledge, G.C. (2001) Experimental Characterization of Electrospinning: The Electrically Forced Jet and Instabilities, *Polymer*, **42**, 9955-9967. https://doi.org/10.1016/S0032-3861(01)00540-7

[24] Menchaca, E.C., García, C.A., Castañeda, I., García, M.A., Guardián, R. and Uruchurtu, J. (2013) Nylon/Grafene Oxide Electrospun Composite Coating. *Journal of Polymer Science*, Article ID: 621618.

[25] Stankovich, S., Piner, R.D., Nguyen, S.T. and Ruoff, R.S. (2006) Synthesis and Exfoliation of Isocyanate-Treated Graphene Oxide Nanoplatelets. *Carbon*, **44**, 3342-3347. https://doi.org/10.1016/j.carbon.2006.06.004

[26] Starkweather, H.W. and Moynihan, R.E. (1956) Density, Infrared Absorption, and Crystallinity in 66 and 610 Nylons. *Journal of Polymer Science Part A*, **22**, 363-368. https://doi.org/10.1002/pol.1956.1202210202

[27] Proctor, J.E., Gregoryanz, E., Novoselov, K.S., Lotya, M., Coleman, J.N. and Halsall, M.P. (2009) High-Pressure Raman Spectroscopy of Graphene. *Physical Review B*, **80**, Article ID: 073408.

[28] Mattevi, C., Eda, G., Agnoli, S., Miller, S., Mkhoyan, K.A., Celik, O., Mastrogiovanni, D., Granozzi, G., Garfunkel, E. and Chhowalla, M. (2009) Evolution of Electrical, Chemical, and Structural Properties of Transparent and Conducting. *Advanced Functional Materials*, **19**, 2577. https://doi.org/10.1002/adfm.200900166

[29] Lopez, V., Sundaram, R.S., Gomez-Navarro, C., Olea, D., Burghard, M., Gomez-Herrero, J., Zamora, F. and Kern, K. (2009) Chemical Vapor Deposition Repair of Graphene Oxide: A Route to Highly-Conductive Graphene Monolayers. *Advanced Materials*, **21**, 4683.

[30] Xu, J.S., Zhang, J. and Liu, X.Y. (2012) Hydrothermal Synthesis of Copper Hydroxyphosphate Hierarchical Architectures. *Chemical Engineering & Technology*, **35**, 2189. https://doi.org/10.1002/ceat.201100698

[31] Yan, C.L., Zou, L.J, Xu, J.S., Wu, J.S., Liu, F., Luo, C. and Xue, D.F. (2008) Chemical Strategy for Tuning the Surface Microstructures of Particles. *Powder Technology*, **183**, 2. https://doi.org/10.1016/j.powtec.2007.11.016

[32] Díaz-Alejo, L.A., Menchaca-Campos, E.C., Uruchurtu-Chavarín, J., Sosa-Fonseca, R. and García-Sánchez, M.A. (2013) Effects of the Addition of Ortho- and Para-NH2 Substituted Tetraphenylporphyrins on the Structure of Nylon 66. *Internacional Journal of Polymer Science*, **2013**, 1-14. https://doi.org/10.1155/2013/323854

[33] Smith, K.M. (1979) Porphyrins and Metalloporphyrins. Elsevier Scientific Publishing Co, Amsterdam.